Available online at www.sciencedirect.com
ScienceDirect
Journal of Chromatography B, 840 (2006) 76–84
JOURNAL OF CHROMATOGRAPHY B
www.elsevier.com/locate/chromb

Purification of VP3 protein of infectious bursal disease virus using nickel ion-immobilized regenerated cellulose-based membranes

Hui-Ling Hu [a], Min-Ying Wang [b], Chiung-Hsuah Chung [a], Shing-Yi Suen [a,*]

[a] *Department of Chemical Engineering, National Chung Hsing University, Taichung 402, Taiwan*
[b] *Graduate Institute of Biotechnology, National Chung Hsing University, Taichung 402, Taiwan*

Received 21 December 2005; accepted 25 April 2006
Available online 22 May 2006

Abstract

In this study, hexa-histidine tagged VP3 protein of infectious bursal disease virus (IBDV) was purified using immobilized metal ion affinity technique from the fermentation of *Escherichia coli* BL21 (DE3) containing a recombinant plasmid with a VP3 gene. The purification efficiencies of VP3 protein (TVP3 and ΔTVP3) using Ni^{2+}-NTA commercial agarose gels and Ni^{2+}-IDA regenerated cellulose-based membranes at 4 °C were compared. A good washing condition for removing most impurity proteins was found as 20 mM NaH_2PO_4, 500 mM NaCl, 40 mM imidazole, pH 7.8, whereas an efficient elution condition was 20 mM NaH_2PO_4, 500 mM NaCl, 500 or 750 mM imidazole, pH 7.8. By applying these conditions to the flow experiments, similar recovery (86–88%) and purity (98–99%) for VP3 were obtained in both gel column (1 ml gel) and membrane cartridge (four membrane disks) under the flow rate of 1.7 ml/min for protein loading and 2.7 ml/min for protein elution. Regarding that the membrane process exhibited some advantages such as shorter residence time and lower cost, a better process efficiency in a large-scale system could be expected for the Ni^{2+}-IDA membranes.

Keywords: Infectious bursal disease virus; Immobilized metal ion affinity chromatography; Immobilized metal ion affinity membrane; VP3 protein

1. Introduction

Infectious bursal disease virus (IBDV) is the causative agent of a highly contagious immuno-suppressive disease in young chickens (between 3 and 6 weeks of age). The immunosuppression results from a depletion of B lymphocytes [1]. The IBDV genome consists of two segments of double-stranded RNA, designated as A and B of size 3.0 and 3.4 kb, respectively [2]. Segment A encodes a 108 kDa polyprotein that is self-cleaved to produce VPX (48 kDa), VP3 (32 kDa), and VP4 (28 kDa). In the mature virions, VPX is processed into VP2 (41 kDa).

VP3 is a structural group-specific protein of IBDV [3] and has been suggested to be the major immunogenic protein of IBDV because the earliest antibodies that appear after infection with live or inactivated viruses are directed to it [4]. Consequently, recombinant VP3 becomes an important protein which could be applied to detect the antibodies induced by IBDV. To evaluate the feasibility of development of VP3-based enzyme-linked immunosorbent assay (ELISA), methods for economically purifying large quantities of VP3 are explored in the present study.

Among the recently developed purification techniques, immobilized metal affinity chromatography (IMAC) is a promising technique for the purification of recombinant proteins due to its advantages of high recovery, high capacity, and complete regeneration [5–7]. Immobilized metal ion affinity method is based on the affinities between certain metal-binding amino acids in the side chains of proteins (e.g. histidine, cysteine, tyrosine, etc.) [8–10] and the metal ions (e.g. Cu^{2+}, Ni^{2+}, Zn^{2+}, etc.) chelated by the chelating agents (e.g. iminodiacetic acid (IDA), nitrilotriacetic acid (NTA), etc.) [11] immobilized on the solid supports. One topic in recent developments is to adopt the immobilized metal affinity membrane (IMAM) process, instead of using the conventional packed-column chromatographic process, for achieving better mass-transfer performance. The membrane system has the advantages such as negligible diffusion limitation, lower pressure drop, higher accessible flow

* Corresponding author. Tel.: +886 4 2285 2590; fax: +886 4 2285 4734.
E-mail address: sysuen@nchu.edu.tw (S.-Y. Suen).

1570-0232/$ – see front matter © 2006 Elsevier B.V. All rights reserved.
doi:10.1016/j.jchromb.2006.04.032

rate, simpler design, and easier scale up [12–16]. Up to now, the IMAMs have been successfully applied in isolating or purifying enzymes, albumins, immunoglobulins, hemoglobins, ribonucleases, growth factors, histidine-tagged viruses, etc. [17–19].

In this study, we compared the purification performance of VP3 (named as TVP3 here) and its C-terminally truncated mutant (ΔTVP3) using Ni^{2+}-NTA commercial agarose gels and Ni^{2+}-IDA regenerated cellulose-based membranes. The two recombinant proteins were highly expressed using the pET28 vector system in *Escherichia coli* following the method in Dr. M.-Y. Wang's Lab [20]. Both of them could be purified by the immobilized metal ion affinity method because a hexa-histidine tag was fused at their N-terminal. The optimal operation conditions for both immobilized metal ion affinity matrices (gels and membranes) and the characterization of the purified VP3 proteins were investigated.

2. Experimental

2.1. Materials

Commercial Ni^{2+}-NTA agarose (6% cross-linking) gels were from QIAGEN (Valencia, CA, USA), with the bead size of 60–160 μm. The regenerated cellulose (RC) membranes from Sartorius (Gottingen, Germany), with a diameter of 47 mm, an average pore size of 0.45 μm, and a thickness of 160 μm, were adopted as the solid supports of IMAM. Iminodiacetic acid (IDA), imidazole, and nickel sulfate were obtained from Acros Organics (Geel, Belgium). Kanamycin was from Sigma (St. Louis, MO, USA). Isopropyl-β-D-thiogalactopyranoside (IPTG) was from GERBU (Gaiberg, Germany). Ethylenediaminetetraacetic acid disodium salt dihydrate (EDTA) and epichlorohydrin were purchased from Tedia (Fairfield, OH, USA). Other chemicals were of analytical grade. The recombinant plasmid vector (pET28a), clone of VP3 and anti-VP3 antibodies were provided from Dr. M.-Y. Wang's lab [20].

2.2. Preparation of regenerated cellulose-based IMAM

All the reactions were carried out in a 120 ml glass bottle. A piece of RC membrane disk was incubated in a solution of 5 ml epichlorohydrin at aqueous phase (20 ml of 1 M NaOH) or at alcohol phase (5 ml of 1 M NaOH mixed with 15 ml of 98% ethanol) and shaken under a constant shaking rate at 60 °C for 2 h. After incubation, the membrane was rinsed with deionized (DI) water. Reaction conditions such as shaking rate and epichlorohydrin phase were varied to study their effects on the coupled epichlorohydrin density. For coupling IDA, the epichlorohydrin-conjugated membrane was reacted with 25 ml of 0.2 M IDA and 1 M Na_2CO_3, pH 11, at 80 °C for 12 h. After reaction, the membrane was washed with 5% acetic acid and DI water. Each modified membrane was immersed in 10 ml of 0.05 M $NiSO_4$ solution for 1 h and then rinsed with DI water in order to remove the unbound or weakly bound nickel ions. The reaction scheme has been presented in our previous study [15].

2.3. Expression and preparation of crude TVP3 and ΔTVP3 extract

The cells of *E. coli* BL21 (DE3) plysS which contained a recombinant pET28a plasmid carrying TVP3 or ΔTVP3 gene were grown at 37 °C overnight. One milliliter of the overnight culture was inoculated to 10 ml of fresh Luria-Bertani medium in the presence of 50 μg/ml Kanamycin and grown to OD_{600} of 0.5–0.6 at 37 °C. Protein expression was induced by adding IPTG to a final concentration of 1 mM. After 3 h, the cells were pelleted at 9838 × *g* (Kubota Ra 200-J rotor, Tokyo, Japan) and 4 °C for 20 min and then lysed on ice by an ultrasound in a lysis buffer (20 mM NaH_2PO_4, 500 mM NaCl, 10 mM imidazole, pH 6.6). Cell lysates were centrifuged at 9838 × *g* and 4 °C for 20 min, and the supernatant was collected and stored at −20 °C for further purification.

2.4. Batch purification experiments

For batch experiments, 1 ml of Ni^{2+}-NTA commercial agarose gel (10.21 ± 0.38 μmol Ni^{2+}/ml) or four pieces of Ni^{2+}-IDA RC-based membrane (10.48 ± 0.67 μmol Ni^{2+}/4 disks) were put into a glass bottle and 10 ml of crude protein extract in the lysis buffer was loaded. The incubation was conducted at 4 °C for 1 h. After binding, the glass bottle was washed by 10 ml of loading buffer (lysis buffer) and 10 ml of washing buffer (20 mM NaH_2PO_4, 500 mM NaCl, 40 mM imidazole, pH 7.8). Then, the VP3 proteins were eluted using 2 ml of elution buffer (20 mM NaH_2PO_4, 500 mM NaCl, 500 mM or 750 mM imidazole, pH 7.8). Different imidazole concentrations in the elution buffer were tested in this work.

2.5. Flow purification experiments

For flow experiments at 4 °C, 1 ml of Ni^{2+}-NTA commercial agarose gel or four pieces of Ni^{2+}-IDA RC-based membrane (under the optimal preparation conditions) were employed. The gels were packed as slurry into an acrylic column (1.0 cm diameter) to give a 1.9 cm bed, and the membrane chromatographic system comprised an acrylic 47 mm-membrane cartridge (lab made). Ten milliliters of crude VP3 extract was loaded at a constant flow rate using a peristaltic pump (MP-3N, Eyela, Tokyo, Japan) to the column or cartridge already equilibrated with the lysis buffer. Unbound proteins were then washed out with 10 ml of washing buffer at 2.7 ml/min. Finally, bound proteins were eluted with 2 ml of elution buffer at a constant flow rate. Fractions of the eluate were collected and analyzed by SDS-PAGE and Western blotting.

2.6. Analysis methods

2.6.1. Determination of hydroxyl group content on RC membrane

A piece of RC membrane was dissolved in 10 ml of 2 M HCl at 100 rpm and 90 °C for 4 h. The solution was centrifuged at 9.83 × *g* for 10 min and the supernatant was taken out. 0.5 ml of supernatant was added to 1.5 ml of 1 M NaOH, and the mixture

was diluted using 4 ml DI water. One milliliter of DNS reagent (10 g/l dinitrosalicylic acid, 2 ml/l phenol, 0.5 g/l Na_2SO_3, 10 g/l NaOH) was added to 1 ml of the diluted sample and the reaction was conducted at 96 °C. After 10 min reaction, the absorbance of the solution at 540 nm was measured using the UV–vis spectrophotometer (Hitachi U-2001, Tokyo, Japan). The hydroxyl group concentration in the solution was evaluated from the calibration curve obtained by using glucose as standard.

2.6.2. Determination of epichlorohydrin and IDA densities on RC membrane

The epichlorohydrin and IDA densities were determined by measuring the differences in oxygen and nitrogen contents, respectively, between the original RC membrane and the membrane from the intermediate reaction step using elemental analyzer (EA) (Heraeus F002, Hanau, Germany).

2.6.3. Determination of nickel ion capacity

To determine the immobilized nickel ion capacity, 1 ml of gel or four pieces of IMAM were washed with 10 ml of 50 mM EDTA solution for 15 min to release the bound nickel ions. The nickel ion concentration in EDTA solution was determined using UV–vis at 400 nm [18].

The measurement of leached nickel ion amount during the elution stage was by atomic absorption spectrophotometry (AAS, Analyst 100, Perkin-Elmer, Norwalk, CT, USA).

2.6.4. Determination of total protein and recombinant VP3 protein amounts

Total protein amount in each sample was measured with the Bio-Rad protein assay using bovine serum albumin (BSA) as the standard [16,18]. As to the VP3 protein amount, its band intensity in the stained membrane after Western blotting was quantified using 1D image analysis software (version 3.6, Kodak, Rochester, NY, USA). The VP3 protein purified as described in a previous study [20] was loaded as the standard for calibration.

2.6.5. SDS-PAGE and Western blotting analysis

Protein analysis was done using 12.5% SDS-PAGE gel, according to the method of Laemmli [21]. The samples were resolved on SDS-PAGE and stained with Coomassie blue. For Western blotting analysis, another 12.5% SDS-PAGE gel, without staining, was electrophoretically transferred onto a PVDF membrane at 100 V for 90 min. The nonspecific sites of the PVDF membrane were blocked with non-fat milk and washed thoroughly with phosphate-buffered saline containing Tween 20 (PBST). After blocking, the PVDF membrane was incubated with VP3 polyclonal antibodies. Alkaline phosphatase-conjugated affinipure goat anti-rabbit IgG was used as the second antibody. After washing, the color development method reported by Cheng et al. [22] was adopted.

2.6.6. Gel filtration

The sizes of native TVP3 and ΔTVP3 were determined by using a Sephacryl S-200 HR column connected to the GradiFrac system (Pharmacia Biotech, Uppsala, Sweden). All runs were performed at 4 °C, with a flow rate of 0.5 ml/min. The column was equilibrated with the elution buffer used in purification experiments and calibrated with chymotrypsinogen A (25 kDa), BSA (66 kDa), aldolase (158 kDa), catalase (232 kDa), and blue dextran 2000 (2000 kDa). One milliliter of TVP3 or ΔTVP3 protein (1 mg/ml) was loaded and the mobile phase was the elution buffer. Fractions of 2 ml eluate were collected, and the VP3-containing fractions were detected using ELISA.

2.6.7. ELISA

Polyvinyl chloride 96-well plates (EIA/RIA strip plate, Costar, Cambridge, MA, USA) were coated with the fractions collected from gel filtration measurement in a carbonate-bicarbonate buffer (pH 9.6) overnight at room temperature. After absorption, the plates were washed three times with PBST, and then 200 μl blocking reagent (5% skim milk in PBS) was added to each well. After overnight incubation at 4 °C, the plates were washed with PBST three times. The plates were treated with horseradish peroxidase (HRP)-conjugated goat anti-rabbit IgG (Jackson ImmunoResearch Laboratories, West Grove, PA, USA) diluted to 1:5000 in PBST buffer for 2 h at 4 °C. Following wash, 100 μl *o*-phenylenediamine dihydrochloride (OPD) substrate solution (Sigma) was added to each well, and the plates were incubated for 7 min for color development. After adding 50 μl of 3 M HCl to stop reaction, the absorbance values were measured at 490 nm with an ELISA reader (Dynex Technologies, Chantilly, VA, USA).

3. Results and discussion

3.1. Regenerated cellulose-based IMAM

Because of their high-degree hydrophilicity, low nonspecific protein adsorption, chemical and mechanical resistances, as well as enough reactive functional groups for ligand immobilization, RC membranes are a good choice as the base materials for the preparation of IMAMs. In the previous studies [15,16,19], the basic adsorption properties for the RC-based IMAMs have been extensively investigated and the possible binding mechanisms discussed. Moreover, practical applications for these RC-based IMAMs have also been explored by evaluating their efficiencies on penicillin G acylase (PGA) purification process [16,19] and VP2 purification process [18].

As reported by Wu et al. [15] for the RC-based IMAMs, the highest copper ion capacity and protein adsorption capacity were achieved when IDA was adopted as the chelator. Moreover, a suitable NTA reagent is not easy to get from commercial sources. Hence, IDA was selected in this study. Based on the literature about immobilized metal affinity methods [16,23,24], the coupled IDA density could be greatly influenced by various reaction conditions such as pH, temperature, concentration, coupling time, shaking rate, etc. Among these factors, shaking rate was almost never mentioned or considered as an important effect dominating the immobilization performance. However, in a previous study [16] shaking rate was found to greatly influence the immobilized metal ion capacity when epichlorohydrin was adopted to react with both the hydroxyl groups of RC membrane

Table 1
Capacity results using different phases in the epichlorohydrin coupling step with different shaking rates

Capacity (μmol/disk)									
Shaking rate (rpm)	Residual group on the membrane	Aqueous phase for epichlorohydrin coupling				Alcohol phase for epichlorohydrin coupling			
		RC	RC-epi	RC-epi-IDA	RC-epi-IDA-Ni^{+2}	RC	RC-epi	RC-epi-IDA	RC-epi-IDA-Ni^{+2}
50	Hydroxyl group	493.07 ± 0.73				493.07 ± 0.73			
100	Epichlorohydrin		96.46 ± 0.35 (19.6%)				129.31 ± 0.29 (26.2%)		
100	IDA			13.64 ± 0.72 (14.1%)				21.50 ± 0.88 (16.6%)	
100	Nickel ion[a]				2.22 ± 0.03 (16.3%)				2.62 ± 0.05 (12.2%)
100	Epichlorohydrin		151.76 ± 0.65 (30.8%)				164.98 ± 0.39 (33.5%)		
100	IDA			21.24 ± 0.32 (14.0%)				23.69 ± 0.44 (14.4%)	
100	Nickel ion[a]				2.72 ± 0.05 (12.8%)				2.75 ± 0.02 (11.6%)

epi: epichlorohydrin. The percentage (%) was the utilization percentage for each reaction step.
[a] The nickel ion capacity was measured using UV–vis at 400 nm.

and the IDA reagent. The main reason is that epichlorohydrin is water-insoluble and it would distribute in the aqueous solution as oil drops. Without any external force, epichlorohydrin drops hardly touched the membrane surface since they were surrounded by water. When shaking rate was raised, epichlorohydrin drops would get more chances to contact the membrane surface and hence be able to react with the hydroxyl groups on the RC membrane. That is, the use of higher shaking rate would mainly improve the mass transfer rate of epichlorohydrin drops from the aqueous solution to the membrane surface. High shaking rate effect on the improvement for the diffusion of IDA molecules or metal ions, as mentioned in the previous study [16], seems not the dominant mechanism.

To verify whether the above postulation is correct, the epichlorohydrin reagent was dissolved in 98% ethanol and the whole metal ion immobilization procedures were repeated in this study. The resulted capacities after each reaction procedure are presented in Table 1. Even using lower shaking rate (50 rpm), epichlorohydrin could be totally dissolved in the alcohol phase and its mass transfer to the membrane surface was no longer restricted by the water phase. Hence, the coupled epichlorohydrin and IDA capacities were greatly increased, when comparing to the results using the aqueous phase for reaction under the same shaking rate. The final nickel ion capacity in this case was 18% more than that for aqueous phase. When the shaking rate was raised to 100 rpm, the mass transfer rate of epichlorohydrin drops from the aqueous solution to the membrane surface was accelerated so that the drops could get sufficient opportunity to touch and react with the residual hydroxyl groups on the membrane. Accordingly, closer values were obtained for the coupled epichlorohydrin, IDA, and nickel ion capacities in both cases under high shaking rate.

In the case using aqueous phase for epichlorohydrin coupling, the coupled epichlorohydrin capacity for shaking rate of 100 rpm was 57% higher than that for 50 rpm, while the final nickel ion capacity was 23% more. When using alcohol phase, the coupled epichlorohydrin capacity and immobilized nickel ion capacity for 100 rpm were 28 and 5%, respectively, more than those for 50 rpm. These results indicate that shaking rate effect was less significant for the employment of alcohol phase.

It should be noted that an optimal shaking rate was reported as 150 rpm in the previous study [16] for the copper ion-immobilized membranes. In this study, when the shaking rate was further raised to 150 rpm, the resulting nickel ion capacity on the membrane was almost identical to that for 100 rpm. Therefore, 100 rpm was adopted to prepare the IMAMs for the subsequent experiments. Moreover, with regard to reducing the organic solvent consumption, the aqueous-phase reaction was employed under this shaking rate.

It is also worth noting that the utilization percentage for each reaction step (capacity obtained for the current reaction step/capacity for the earlier one step) was low (as shown in Table 1), which may cause unnecessary nonspecific binding and reduce the applicability of IMAMs. In order to resolve this problem, suitable methods for blocking the unreacted residual groups, i.e. hydroxyl group, epoxide group, and carboxyl group, are necessary. For example, the epoxy groups could be blocked

Table 2
VP3 purification performance in the batch process

Stage	ΔTVP3					TVP3				
	Volume (ml)	Total protein (mg)	ΔTVP3 (mg)	ΔTVP3 recovery (%)	Purification fold	Volume (ml)	Total protein (mg)	TVP3 (mg)	TVP3 recovery (%)	Purification fold
Ni^{2+}-NTA gels										
Crude lysate	10	19.13	1.51	–	–	10	17.41	1.46	–	–
Residue	10	16.43	0.02	0.99	0.01	10	13.90	0.02	1.44	0.02
Wash (10 mM imidazole; pH 6.5)	10	1.18	0.01	0.53	0.06	10	1.98	0.01	0.83	0.08
Wash (40 mM imidazole; pH 7.8)	10	0.03	0.02	0.19	3.62	10	0.12	0.03	2.34	3.36
Elution (500 mM imidazole; pH 7.8)	10	1.50	1.47	97.29	12.42	10	1.41	1.39	95.40	11.78
Elution (750 mM imidazole; pH 7.8)	10	0.00	0.00	0.20	12.66	10	0.00	0.00	0.14	11.94
Ni^{2+}-IDA membranes										
Crude lysate	10	18.64	1.53	–	–	10	17.89	1.47	–	–
Residue	10	15.94	0.01	0.33	0.01	10	14.41	0.01	0.68	0.01
Wash (10 mM imidazole; pH 6.5)	10	1.15	0.00	0.08	0.01	10	1.99	0.01	0.54	0.05
Wash (40 mM imidazole; pH 7.8)	10	0.01	0.00	0.20	0.04	10	0.04	0.00	0.28	1.28
Elution (500 mM imidazole; pH 7.8)	10	1.00	0.99	64.86	12.07	10	1.03	0.98	66.78	11.61
Elution (750 mM imidazole; pH 7.8)	10	0.54	0.54	35.14	12.18	10	0.48	0.47	32.07	12.08

All experiments were repeated twice.

with mercaptoethanol in refs. [25,26]. However, it is difficult to find a simple blocking agent to block all these three different groups simultaneously. Alternatively, a simple washing step was adopted in this work to remove the impurity proteins adsorbed by nonspecific binding (as described in Section 3.2). In addition, the nickel ion capacity obtained in this study may not be the optimal value because the immobilization step only underwent for 1 h. Longer time duration for coupling nickel ion may further raise the nickel ion capacity.

3.2. Purification performance in the batch process

Both the Ni^{2+}-NTA commercial agarose gels and Ni^{2+}-IDA RC-based membranes were used for the batch purification of VP3 and some operation conditions were selected to achieve higher purification efficiency. One milliliter of Ni^{2+}-NTA commercial agarose gel and four pieces of Ni^{2+}-IDA RC-based membrane were employed because their Ni^{2+} capacities were very close.

3.2.1. Selection of buffers

The results from batch experiments are listed in Table 2. After loading the crude protein lysate onto the affinity column or membrane holder, a few proteins other than VP3 were also bound to the column or membranes specific or nonspecific. In order to reduce the binding of these impurity proteins, the lysis buffer with 10 mM imidazole and pH 6.5 was adopted directly as the loading buffer and most of VP3 proteins were adsorbed (more than 98%). When applying this lysis buffer for washing, only few VP3 but some impurity proteins were washed out. When further applying the buffer with 40 mM imidazole and pH 7.8 for the second washing, a small amount of impurity proteins was removed.

The VP3 could be entirely eluted out with the use of 500 mM imidazole, pH 7.8 for the commercial gels, but the assistance of higher-concentration (750 mM) imidazole buffer was necessary for a clear VP3 elution from the IMAMs. This phenomenon could be explained as a result of the stronger binding between the tridentate IDA-chelated Ni^{2+} and the VP3 proteins in the membrane system, compared to that between the tetradentate NTA-chelated Ni^{2+} and the proteins in the gels. About 11–12-fold purification and 95–98% VP3 recovery were achieved by using both matrices in the batch process (Table 2).

3.2.2. Nonspecific binding

The specific binding for protein adsorption onto the IMAC or IMAM could be categorized into two interactions [15]: (1) the affinity binding provided by the electron-donating capacity of the imidazole groups of the exposed histidine residues on the protein surface with the immobilized metal ions; and (2) the electrostatic interaction between the charged protein molecules and positively charged metal ions. Other interactions, such as the electrostatic and hydrophobic interactions between the proteins and the residual groups on the solid matrices, are considered as the nonspecific bindings. To evaluate the nonspecific binding effect in this study, the RC membranes from each intermediate reaction step before complete metal ion immobilization and the NTA-agarose gels without metal ion immobilization were employed in the batch VP3 adsorption. The results of adsorbed VP3 amount are presented in Fig. 1.

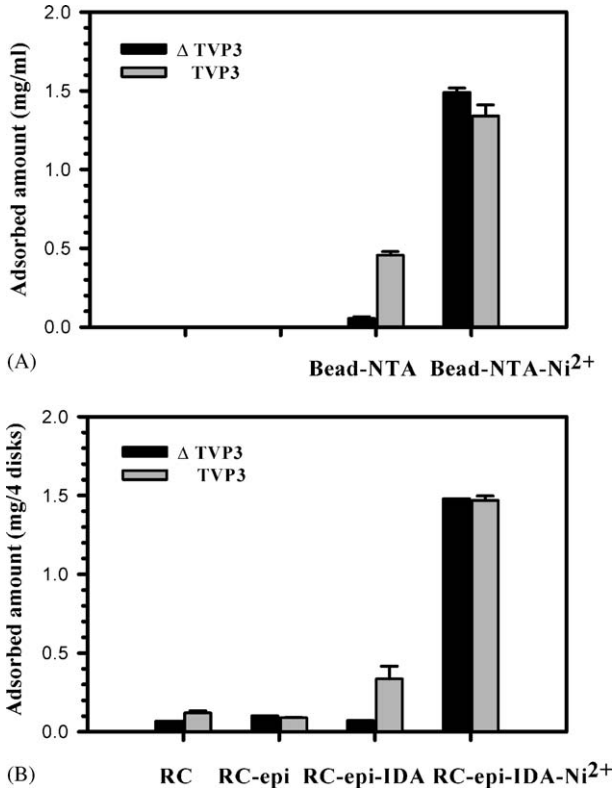

Fig. 1. VP3 adsorption onto different gels (A) and membranes (B).

The nonspecific binding results for blank RC and epichlorohydrin-coupled membranes were small (less than 8.2% of the adsorbed amount for immobilized metal ion membranes). When the chelator was conjugated, the nonspecific binding of ΔTVP3 was still insignificant, but it became important for TVP3. The nonspecific TVP3 binding amount on the chelator-conjugated matrix was about 22.9% for the Ni^{2+}-IDA membranes and 34% for the Ni^{2+}-NTA gels. At pH 6.5, TVP3 protein (pI = 6.06) is slightly cationic, and ΔTVP3 protein (pI = 4.97) is anionic. Since the residual carboxyl groups (p$K_a \approx 3$) [15] on the chelator (either NTA or IDA)-coupled gels or membranes are anionic, the anionic ΔTVP3 would be repelled from them. On the other hand, slightly cationic TVP3 protein could undergo electrostatic interaction with the chelator-coupled gels or membranes, which may explain the obvious TVP3 adsorption onto the chelator-coupled matrices. Besides, the nonspecific binding of TVP3 proteins to the NTA-coupled gels was slightly greater than the IDA-coupled membranes. This phenomenon may be attributed to the fact that the tetradentate chelator NTA has more residual carboxyl groups than tridentate IDA.

It should be noted that either the nonspecific binding of other proteins with the residual functional groups on the affinity matrices or the competitive specific binding of those proteins containing surface histidines with the immobilized metal ions may cause a reduction in the purity of products. Regarding the low utilization percentages for coupling epichlorohydrin, IDA, and Ni^{2+} onto RC membranes in Table 1, the nonspecific binding may not be neglected. As shown in Table 2, about 58–59% adsorption came from the impurity proteins in the TVP3 cases, while 44–45% for the ΔTVP3 cases. Fortunately, most of the adsorbed impurity proteins (95–100%) could be easily washed out using low-concentration imidazole buffer. Therefore, high-purity products could still be obtained even though the residual groups on the affinity matrices were not blocked.

3.3. Purification performance in the flow process

3.3.1. Effect of flow rate

The purification performance of VP3 using the affinity gel column or membrane cartridge at different flow rates is shown in Table 3. Proper binding of the target protein to the immobi-

Table 3
VP3 purification performance in the flow process at different flow rates

Flow rate (ml/min)	ΔTVP3						TVP3					
	Ni^{+2}-NTA gels			Ni^{+2}-IDA membranes			Ni^{+2}-NTA gels			Ni^{+2}-IDA membranes		
	Total time (min)	Recovery (%)	Purity (%)	Total time (min)	Recovery (%)	Purity (%)	Total time (min)	Recovery (%)	Purity (%)	Total time (min)	Recovery (%)	Purity (%)
(1) Loading 0.5 Washing 1.0 Elution 1.0	58.0	93.6	100.0	50.0	91.3	100.0	57.7	92.1	100.0	49.2	90.4	100.0
(2) Loading 1.0 Washing 1.7 Elution 1.7	32.4	90.2	99.6	27.6	89.7	99.3	31.9	89.7	99.9	26.4	88.8	99.1
(3) Loading 1.7 Washing 2.7 Elution 2.7	20.2	88.5	99.0	17.9	87.1	98.7	19.4	87.4	99.3	17.0	86.5	98.4
(4) Loading 2.3 Washing 3.0 Elution 3.0	17.6	64.6	98.2	15.9	62.4	98.0	16.7	63.5	98.4	15.1	62.0	98.2

Protein loading: 10 ml, 1.51 mg/ml. Loading buffer: 20 mM NaH_2PO_4, 500 mM NaCl, 10 mM imidazole, pH 6.5. Washing buffer: 20 mM NaH_2PO_4, 500 mM NaCl, 40 mM imidazole, pH 7.8. Elution buffer: 20 mM NaH_2PO_4, 500 mM NaCl, 500 mM imidazole for gels or 750 mM imidazole for membranes, pH 7.8. All experiments were repeated twice.

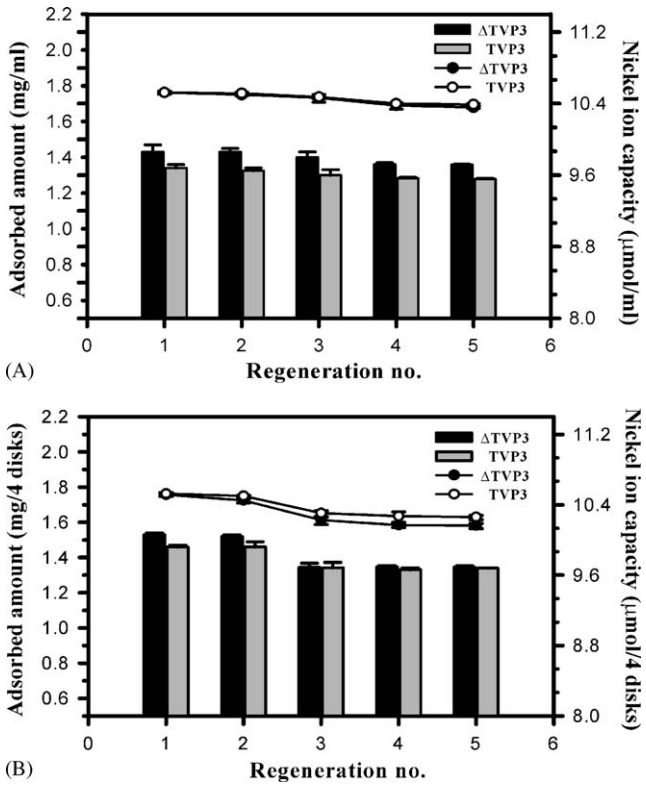

Fig. 2. Regeneration results for Ni^{2+}-NTA gels (A) and Ni^{2+}-IDA membranes (B) in the flow process. Flow rates: loading 1.7 ml/min, washing and elution 2.7 ml/min. The nickel ion capacity was measured using UV–vis at 400 nm.

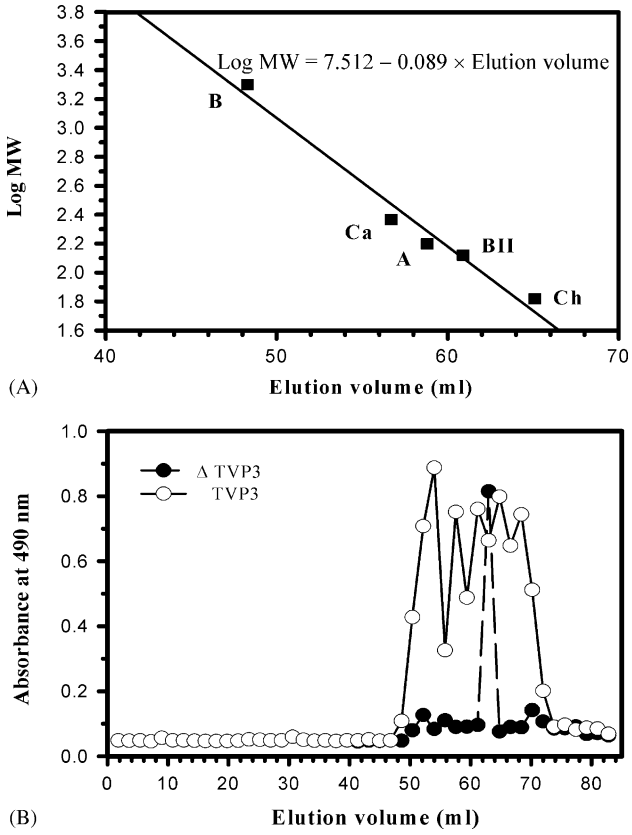

Fig. 3. Gel filtration analysis of purified TVP3 and ΔTVP3 proteins (1 mg/ml). (A) Calibration with blue dextran 2000 (B, 2000 kDa), catalase (Ca, 232 kDa), aldolase (A, 158 kDa), BSA (BII, 66 kDa), and chymotrypsinogen A (Ch, 25 kDa). (B) The fractions were detected on an ELISA reader at 490 nm.

lized metal ions requires sufficient time to attain equilibrium. At comparatively higher flow rates (such as 2.3 and 3 ml/min), the loaded protein did not get enough time for binding, and therefore the recovery of VP3 was low (62–65%). When the flow rate was decreased, the VP3 recovery increased. The optimum flow rate was found to be 1.7 ml/min for protein loading and 2.7 ml/min for protein washing or elution, because the increase in recovery for further lower flow rates was not significant.

Moreover, both matrices obtained similar recovery and purity results as shown in Table 3. Regarding that the IMAM process could offer simpler design, shorter process time (12% lower process time than for IMAC), and lower pressure drop, its process efficiency in a larger-scale system should be superior to the gel bead column. Therefore, VP3 purification with IMAMs is a potential approach in industry.

3.3.2. Regeneration of the immobilized metal ion affinity matrices

The reusabilities of agarose-based IMAC and RC-based IMAM in the flow process were investigated. After VP3 desorption from the IMAC or IMAM, some retained proteins need to be removed for regenerating the IMAC or IMAM. A strong eluent EDTA was used for this purpose. In this work, 10 ml of 50 mM EDTA was adopted for both affinity matrices. After that, the matrices were immersed in 10 ml of 0.05 M $NiSO_4$ solution for 1 h to immobilize the metal ions and regain their affinity power. The regeneration was repeated five times and the relative results are shown in Fig. 2.

The protein adsorption capacity decreased slightly in the third regeneration, yet was stable from the fourth to the fifth time. Same tendency could be observed for the immobilized nickel ion capacity. That is, the reduction in nickel ion immobilization in the regeneration process caused the reduction in protein adsorption capacity. Moreover, the reduction in immobilized nickel ion capacity was more serious for the IMAMs than the gel beads, which possibly resulted from the weaker coupling between the tridentate chelator IDA and nickel ions in the membrane system. In summary, 88% performance efficiency could still be attained after five-time regeneration for the IMAM system, whereas 95% for the IMAC system.

3.4. Characterization of purified VP3 protein

3.4.1. Native size

To determine the multimeric forms of purified TVP3 and ΔTVP3 in vitro, a gel filtration experiment was performed based on the procedures in refs. [27–29]. Only one ΔTVP3-containing peak, but five TVP3-containing peaks, were obtained in the chromatogram (Fig. 3). The molecular mass for ΔTVP3 was calculated to be about 81 kDa, according to the calibration curve with standard proteins, so that it seemed to form trimer (molecular weight of ΔTVP3 monomer ≈ 26 kDa). On the other hand, TVP3-containing peaks corresponded to the molecular masses of approximately 32, 56.4, 117.8, 246, and 2000 kDa. There-

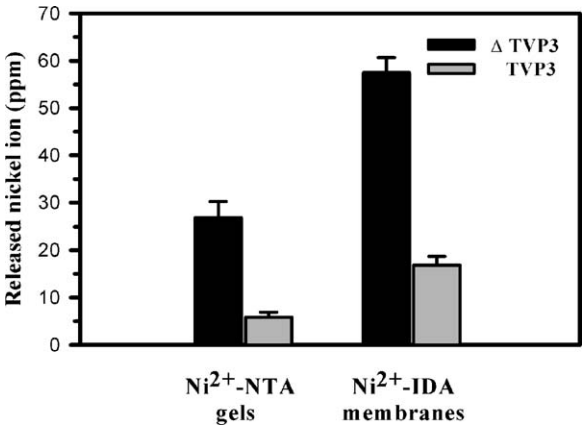

Fig. 4. The released Ni^{2+} concentration during the elution stage of VP3 in the flow purification process. The nickel ion concentration was measured using AAS.

fore, TVP3 could have formed the oligomers (molecular weight of TVP3 monomer ≈ 32 kDa).

3.4.2. *Effect of nickel ion leakage*

The AAS analysis for nickel ion leaching in the elution stage of IMAC and IMAM is shown in Fig. 4. The nickel ion release during elution stage was more pronounced for Ni^{2+}-IDA RC-based membranes than Ni^{2+}-NTA agarose gels, despite almost identical amount of nickel ion immobilized on both absorbents. It may be attributed to two possible reasons: one is that the coupling between the tridentate chelator IDA and nickel ions in the membrane system was weaker than that between the tetradentate chelator NTA and nickel ions in the gel system. The other is that a harsher elution condition (750 mM imidazole) was employed in the membrane system. This may cause the leaching of unstably immobilized metal ions.

In comparison with the amount of leached nickel ions (about 12–18 ppm) reported in ref. [30] using IMAC to purify the recombinant GST-His_6 protein, our results in the TVP3 case are close to theirs. However, more serious nickel ion leaching occurred for ΔTVP3 purification. A probable explanation is that the binding between ΔTVP3 and the immobilized nickel ions could be stronger than that for TVP3 (partly because anionic ΔTVP3 was preferably interacted with Ni^{2+}; partly due to a structural variation between ΔTVP3 and TVP3). Consequently, more unstably immobilized nickel ions were released due to the capture of ΔTVP3.

As reported in ref. [30], the oligomerization of proteins could be induced by the nickel ions leached from the IMAC column. To determine if the ΔTVP3 trimer and the TVP3 oligomers in this study were induced by the nickel ion leaching or not, the purified VP3 proteins were treated at different conditions and the results are shown in Fig. 5. Lane 2 is the SDS-PAGE result for the VP3 proteins purified by IMAC or IMAM in this work. Lane 3 is the result for the purified VP3 sample treated by boiling. Under this treatment, the VP3 proteins were denatured and the oligomers were dissociated to monomers or even smaller residues. Lane 1 is the result for the purified VP3 sample treated with 100 mM EDTA. According to the previous study [30], the oligomerized

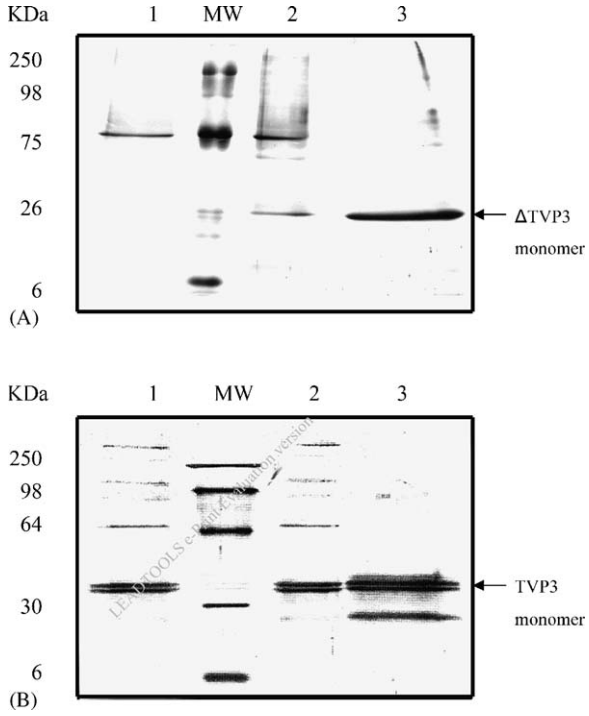

Fig. 5. Oligomerization of the purified TVP3 (A) and ΔTVP3 (B) proteins analyzed by SDS- PAGE. Lane 1: the purified protein sample treated with 100 mM EDTA. Lane 2: the purified protein sample. Lane 3: the purified protein sample under denaturing condition (by boiling).

form of VP3 proteins caused by the surrounded metal ions which were released from IMAC could be decomposed due to the chelation of metal ions with the added EDTA. Consequently, VP3 returned to the original monomer form. However, in this case, the addition of EDTA did not change the oligomeric form of VP3. As shown in Fig. 5, the SDS-PAGE bands in Lane 1 are almost identical to those for Lane 2. Accordingly, the oligomerization of VP3 proteins in the purification process should not be attributed to the induction by the leached nickel ions in this study. Instead, the VP3–VP3 interaction during the purification process may be the main effect.

4. Conclusions

The purification efficiencies of VP3 using the prepared Ni^{2+}-IDA RC-based membranes and the commercially available Ni^{2+}-NTA agarose gels were compared in this study. The optimal operation conditions for high-degree VP3 purification were selected, which are 20 mM NaH_2PO_4, 500 mM NaCl, 10 mM imidazole, pH 6.5 for loading and 20 mM NaH_2PO_4, 500 mM NaCl, 500 or 750 mM imidazole, pH 7.8 for elution. In the flow process, when the flow rate of 1.7 ml/min for loading and 2.7 ml/min for elution were adopted, 86–88% recovery and 98–99% purity could be obtained for both kinds of matrices. Furthermore, 88–95% reusability could be performed after five-time regeneration. From the economic viewpoint, the membrane process has the advantages of lower pressure drop, shorter residence time (it could cut down 12% of the process time for the column system in this work), lower cost (its cost on matrix and chemicals was

one-third of that for resins), simpler design, and easier scale-up, compared to the gel column process. This implies that, in large-scale purification process in the related industries, the IMAMs should be a proper design and it is worth applying in more widespread applications.

From the characterized sizes of the purified VP3 proteins, TVP3 seemed to form oligomers and ΔTVP3 could form trimers. Moreover, these multimeric forms were not induced by the nickel leaching from the IMAC or IMAMs.

As described in previous IBDV studies [31–33], the infection of chickens by IBDV could cause serious economic losses in the poultry industry worldwide, either by causing a high-mortality acute condition or by leading to immunosuppression in young chickens. Detection of antibodies to IBDV has been accomplished by a number of different assays, and ELISA is the most often used method because it is economical and can quickly test large numbers of samples [34]. Commercial ELISA kits are presently available to detect antibodies for IBDV in field samples. The antigen sources for these kits are based on the whole virion [35], which is usually purified through a cesium chloride gradient by ultracentrifugation [36]. However, it leads to high cost and time consumption. To further explore the application of the pure VP3 proteins produced using the expression method [20] and the optimal IMAM or IMAC process established in this study, they have been employed to develop a detection kit for IBDV identification in Dr. M.-Y. Wang's lab. The development is successful and the cost of the kit is relatively low. The related results will be published in the near future.

Acknowledgment

The authors would like to thank Ms. Kai-Ling Fu for her help with the analysis of nickel ion concentration by AAS.

References

[1] E. Burkhardt, H. Muller, Arch. Virol. 94 (1987) 297.
[2] P. Dobos, B.J. Hill, R. Hallett, D.T.C. Kells, H. Becht, D. Teninges, J. Virol. 32 (1979) 593.
[3] H. Becht, H. Muller, H.K. Muller, J. Gen. Virol. 69 (1979) 631.
[4] K.J. Fahey, I.J. O'Donnell, A.A. Azad, J. Gen. Virol. 66 (1985) 1479.
[5] V. Gaberc-Porekar, V. Menart, J. Biochem. Biophys. Methods 49 (2001) 335.
[6] G.S. Chaga, J. Biochem. Biophys. Methods 49 (2001) 313.
[7] E.K.M. Ueda, P.W. Gout, L. Morganti, J. Chromatogr. A 988 (2003) 1.
[8] F.H. Arnold, Bio/Technology 9 (1991) 151.
[9] R.H. Clemmitt, H.A. Chase, Biotechnol. Bioeng. 67 (2000) 206.
[10] W.-S. Choe, R.H. Clemmitt, H.A. Chase, A.P.J. Middelberg, J. Chromatogr. A 953 (2002) 111.
[11] E. Hochuli, W. Bannwarth, H. Dobeli, R. Gentz, D. Stuber, Bio/Technology 6 (1988) 1321.
[12] D.K. Roper, E.N. Lightfoot, J. Chromatogr. A 702 (1995) 3.
[13] C. Charcosset, J. Chem. Technol. Biotechnol. 71 (1998) 95.
[14] Y.-H. Tsai, M.-Y. Wang, S.-Y. Suen, J. Chromatogr. B 766 (2002) 133.
[15] C.-Y. Wu, S.-Y. Suen, S.-C. Chen, J.-H. Tseng, J. Chromatogr. A 996 (2003) 53.
[16] Y.-C. Liu, C.-C. ChangChien, S.-Y. Suen, J. Chromatogr. B 794 (2003) 67.
[17] S.-Y. Suen, Y.-C. Liu, C.-S. Chang, J. Chromatogr. B 797 (2003) 305.
[18] C.-S. Chen, S.-Y. Suen, S.-Y. Lai, G.R.-L. Chang, T.-C. Lu, M.-S. Lee, M.-Y. Wang, J. Virol. Methods 130 (2005) 51.
[19] Y.-C. Liu, S.-Y. Suen, C.-W. Huang, C.-C. ChangChien, J. Membr. Sci. 251 (2005) 201.
[20] Cheng, Y.-H., Master thesis, Graduate Institute of Biotechnology, National Chung Hsing University, Taichung, Taiwan, 2003.
[21] U.K. Laemmli, Nature 227 (1970) 680.
[22] Y.-S. Cheng, M.-S. Lee, S.-Y. Lai, S.-R. Doong, M.-Y. Wang, Biotechnol. Prog. 17 (2001) 318.
[23] E.S. Hemdan, J. Porath, J. Chromatogr. 323 (1985) 265.
[24] Q. Luo, H. Zou, X. Xiao, Z. Guo, L. Kong, X. Mao, J. Chromatogr. A 926 (2001) 255.
[25] C. Mateo, G. Fernandez-Lorente, E. Cortes, J.L. Garcia, R. Fernandez-Lafuente, J.M. Guisan, Biotechnol. Bioeng. 76 (2001) 269.
[26] C. Mateo, O. Abian, G. Fernandez-Lorente, J. Pedroche, R. Fernandez-Lafuente, J.M. Guisan, A. Tam, M. Daminati, Biotechnol. Prog. 18 (2002) 629.
[27] A. Krop-Watorek, S. Oikawa, Y. Oyama, H. Nakazato, Biochem. Biophys. Res. Commun. 242 (1998) 79.
[28] J.M. Eriksson, E. Haggård-Ljungquist, J. Bacteriol. 182 (2000) 6714.
[29] J.I. Fariña, F. Siñeriz, O.E. Molina, N.I. Perotti, Carbohydrate Polymers 44 (2001) 41.
[30] T. Sprules, N. Green, M. Featherstone, K. Gehring, Biotechniques 25 (1) (1998) 20.
[31] F.S.B. Kibenge, A.S. Dhillon, R.G. Russell, J. Gen. Virol. 69 (1988) 1757.
[32] M.M. Nagarajan, F.S.B. Kibenge, Can. J. Vet. Res. 61 (1997) 81.
[33] T.P. van den Berg, Avian Pathol. 29 (2000) 175.
[34] D.J. Jackwood, K.S. Henderson, R.J. Jackwood, Clin. Diagn. Lab. Immunol. 3 (1996) 456.
[35] J.L. Martìnez-Torrecuadrada, B. Lázaro, J.F. Rodriguez, J.I. Casal, Clin. Diagn. Lab. Immunol. 7 (2000) 645.
[36] I.M. Verma, M.D. Weitzman, Ann. Rev. Biochem. 74 (2005) 711.